Supplementary Information for “Giant multiphononic effects in a perovskite oxide”

Claudio Cazorla

Departament de Física, Universitat Politècnica de Catalunya, Campus Nord B4-B5, Barcelona 08034, Spain

Massimiliano Stengel

Institut de Ciència de Materials de Barcelona, ICMAB–CSIC, Campus UAB, 08193 Bellaterra, Spain and ICREA-Institució Catalana de Recerca i Estudis Avançats, 08010 Barcelona, Spain

Jorge Íñiguez

Materials Research and Technology Department, Luxembourg Institute of Science and Technology (LIST), Avenue des Hauts-Fourneaux 5, L-4362 Esch/Alzette, Luxembourg and Department of Physics and Materials Science, University of Luxembourg, 41 Rue du Brill, L-4422 Belvaux, Luxembourg

Riccardo Rurali

Institut de Ciència de Materials de Barcelona, ICMAB–CSIC, Campus UAB, 08193 Bellaterra, Spain

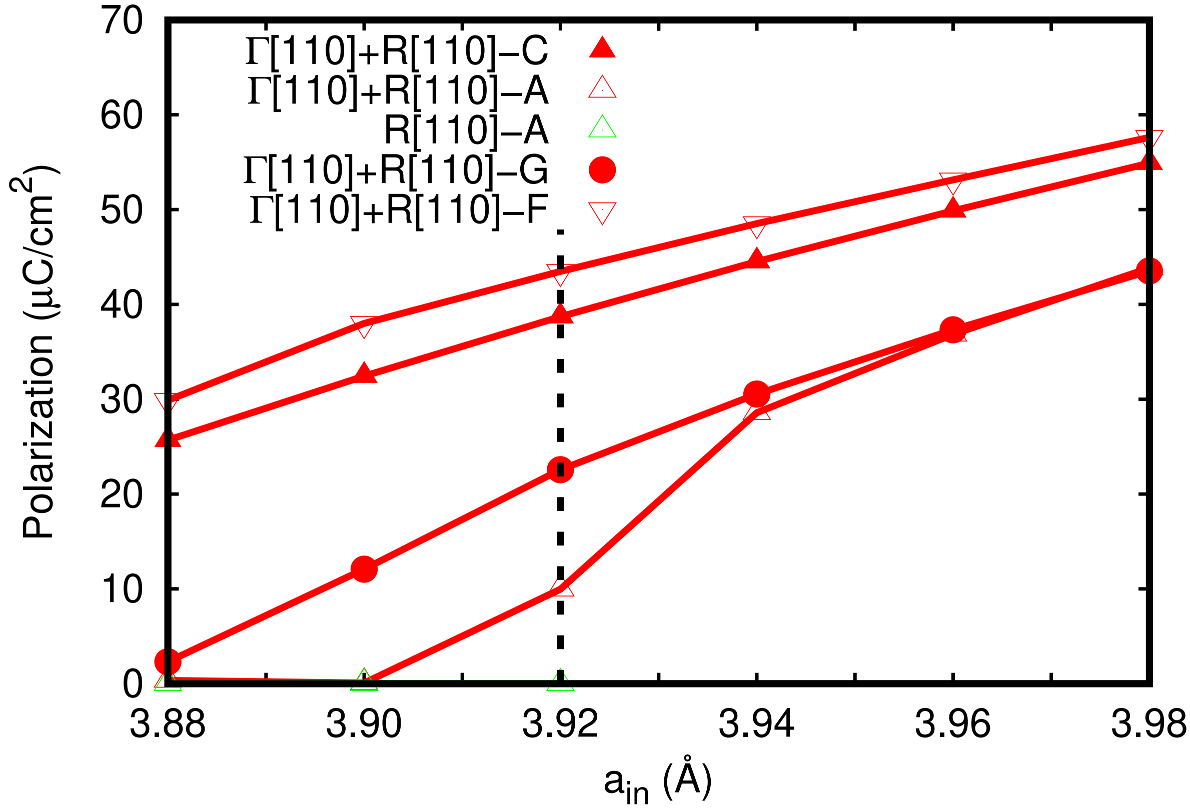

Supplementary Figure 1: Electric polarization of a number of energetically competitive phases in SMO thin films under tensile strains expressed as a function of in-plane lattice parameter. The dotted vertical line marks the occurrence of the magnetoelectric *Ima2*-G → *Ima2*-FM phase transition.

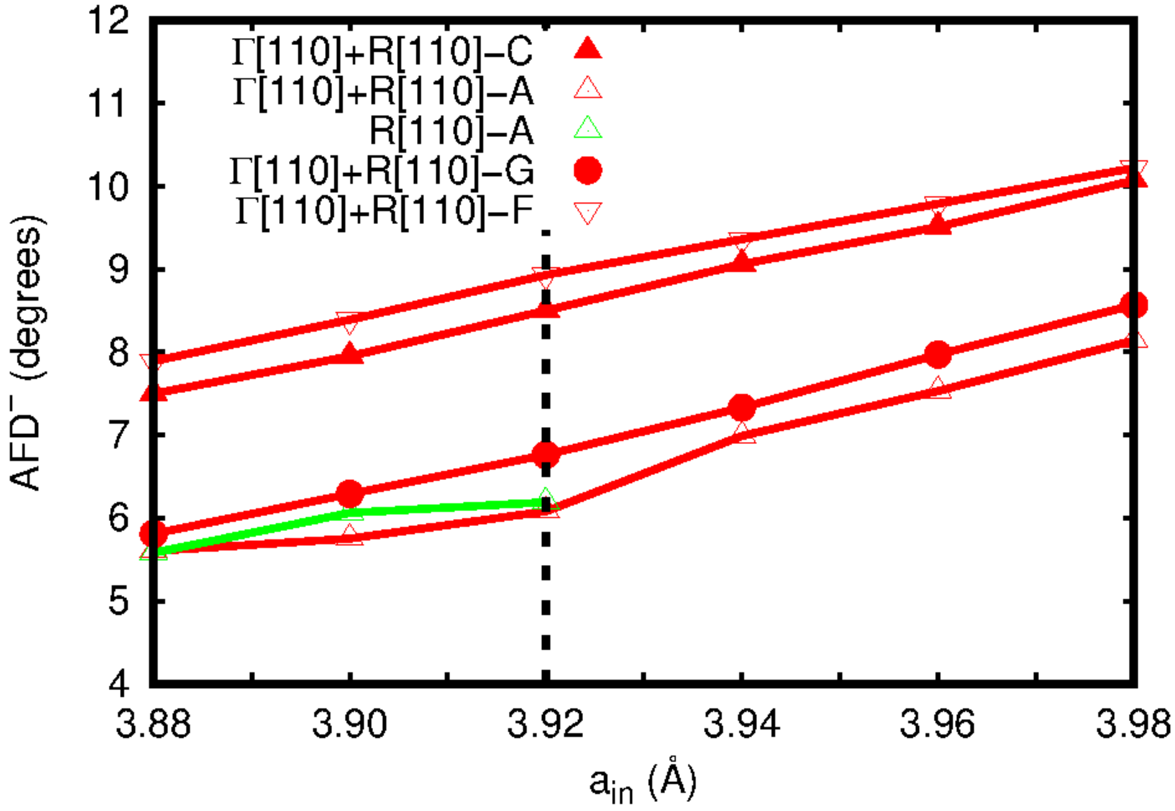

Supplementary Figure 2: Antiphase antiferrodistortive oxygen octahedral rotations (AFD O_6) of the energetically competitive phases of Supplementary Figure 1 expressed as a function of in-plane lattice parameter. The dotted vertical line marks the occurrence of the magnetoelectric *Ima2*-G → *Ima2*-FM phase transition.

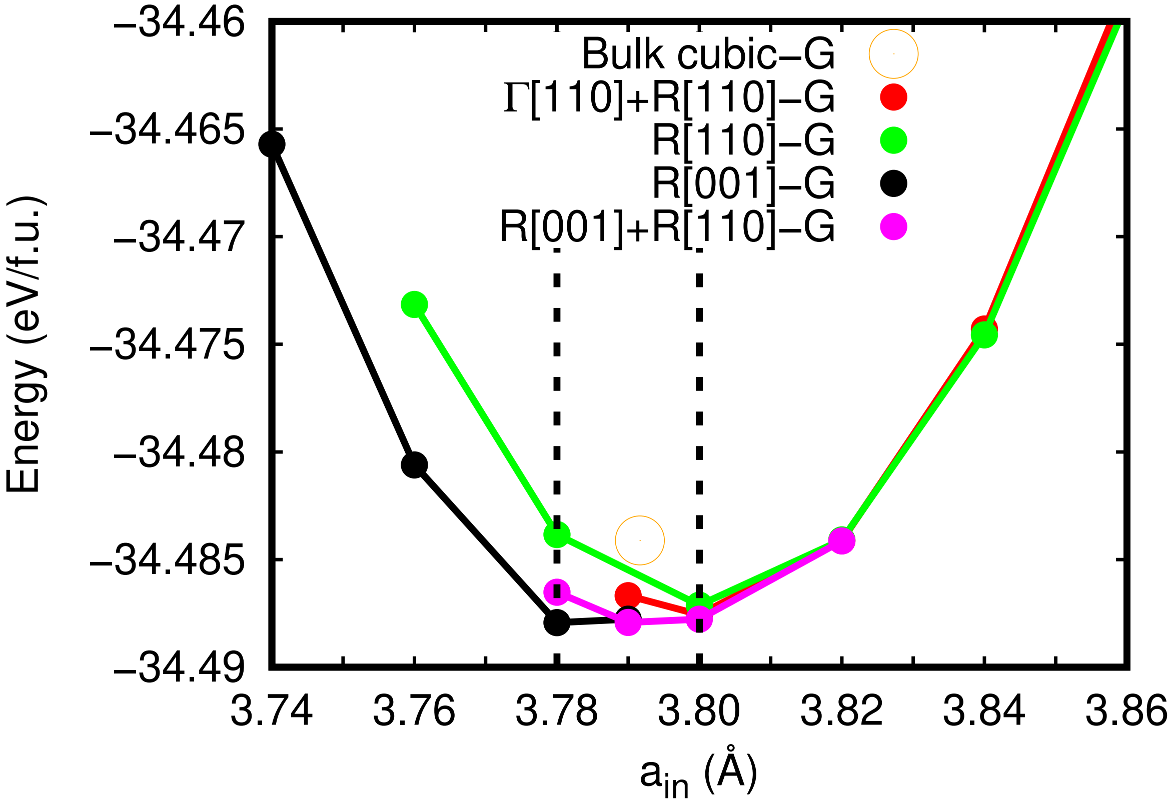

Supplementary Figure 3: Phase diagram of SMO thin films under compressive strains. The dotted vertical lines mark the occurrence of structural phase transitions. The circle represents the energy obtained for bulk SMO in the cubic $Pm\overline{3}m$ structure that is assumed to be its ground state.

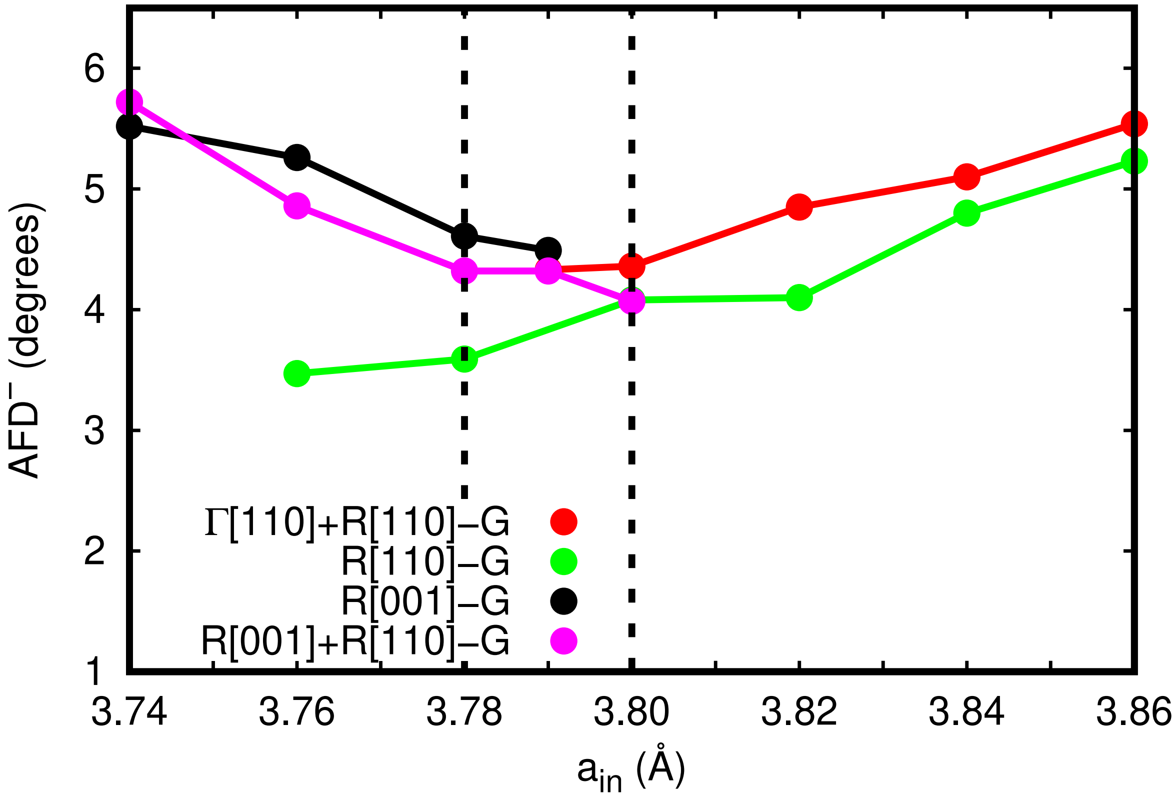

Supplementary Figure 4: Antiferrodistortive oxygen octahedral rotations (AFD O_6) of some energetically competitive phases in SMO thin films under compressive strains expressed as a function of in-plane lattice parameter. The dotted vertical lines mark the occurrence of structural phase transitions. All antiferrodistortive distortions follow out-of-phase patterns (AFD^-).

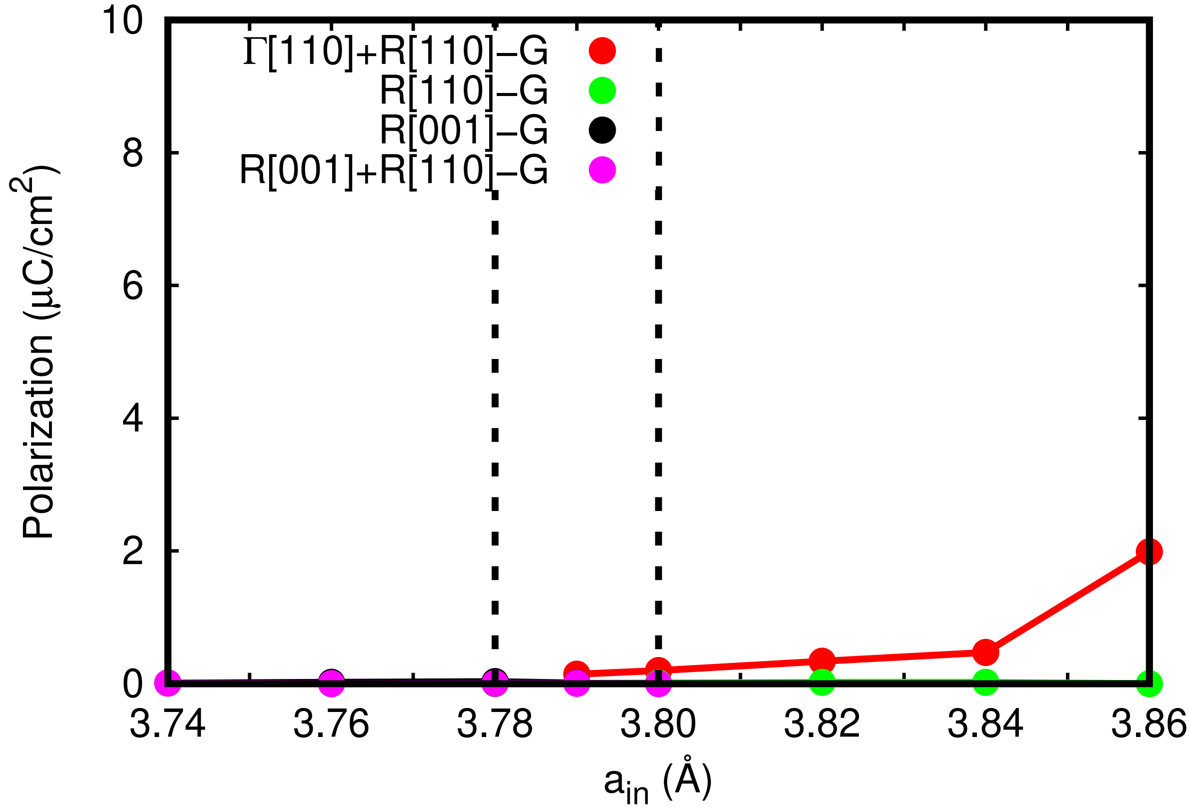

Supplementary Figure 5: Electric polarization of some energetically competitive phases in SMO thin films under compressive strains expressed as a function of in-plane lattice parameter. The dotted vertical lines mark the occurrence of structural phase transitions.

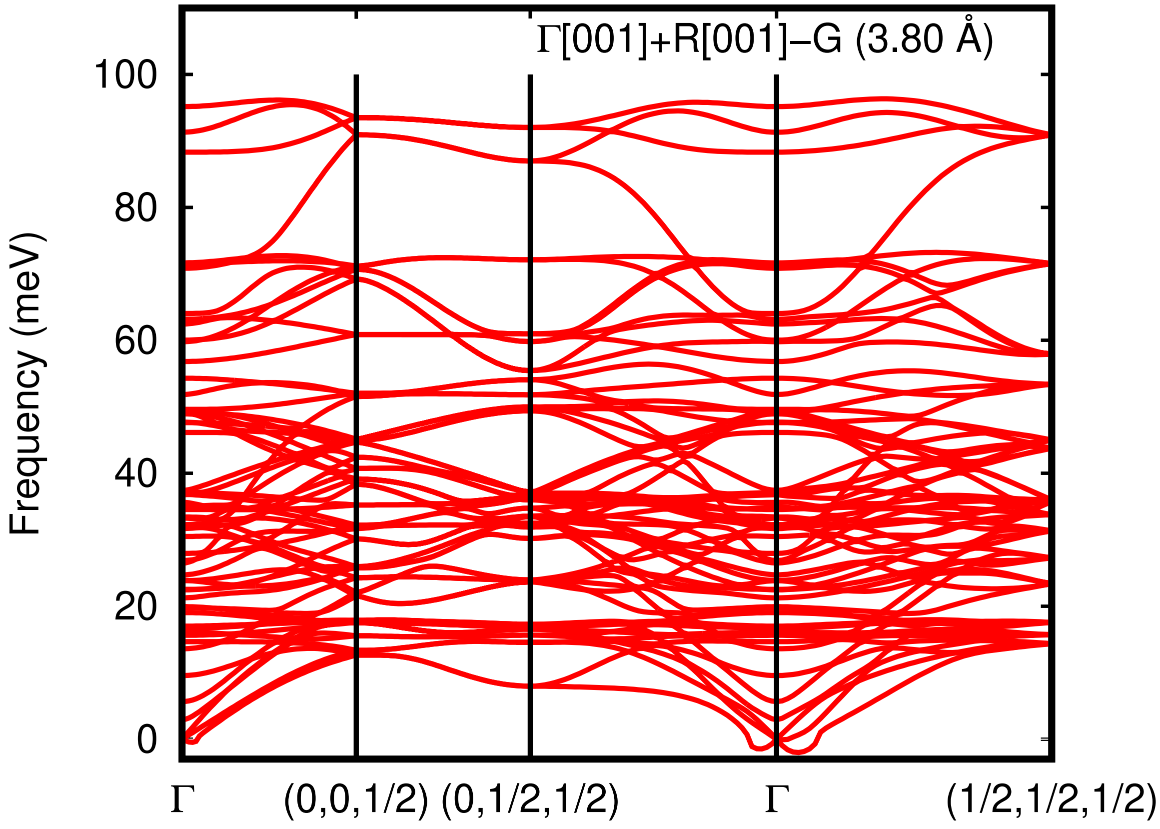

Supplementary Figure 6: Full phonon spectrum of the monoclinic Pc phase that is stabilized within the narrow in-plane lattice parameter interval $3.78 \leq a_{in} \leq 3.80$ Å in SMO thin films.

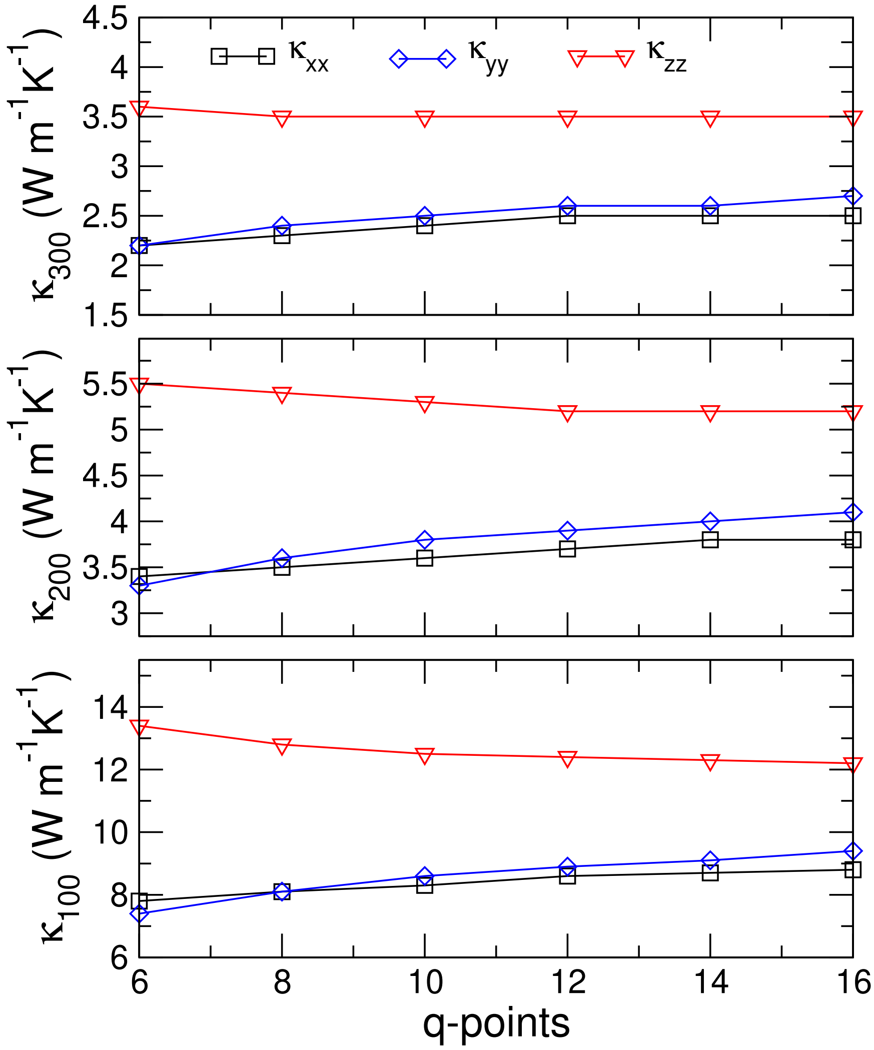

Supplementary Figure 7: Thermal conductivity of the $Ima2$ FM phase at $a_{in} = 3.92$ Å, obtained solving the BTE at the RTA level on different **q**-points grid. Results for $T = 100$, 200, and 300 K (bottom to top) are shown. On the basis of these tests, we adopted a $12 \times 12 \times 12$ grid, which provides converged value within 2%, even at $T = 100$ K where in principle convergence can be slower, due to the importance of long wavelength heat carrying phonons.

	κ_{xx}	κ_{yy}	κ_{zz}
T = 100 K			
RTA	7.8	7.4	13.4
iterative	7.9	7.6	13.6
T= 200 K			
RTA	3.4	3.3	5.5
iterative	3.4	3.4	5.5
T= 300 K			
RTA	2.2	2.2	3.6
iterative	2.3	2.3	3.6

Supplementary Table 1: Comparison between the thermal conductivity obtained from the RTA and from the iterative solution of the BTE at $T = 100$, 200, and 300 K on a $6 \times 6 \times 6$ grid of **q**-points. Corrections to the RTA are negligible and amount, at most, to 2.7% for κ_{yy} at $T = 100$ K. Physically, this suggests that momentum conserving Normal processes are not playing a significant role in phonon transport.

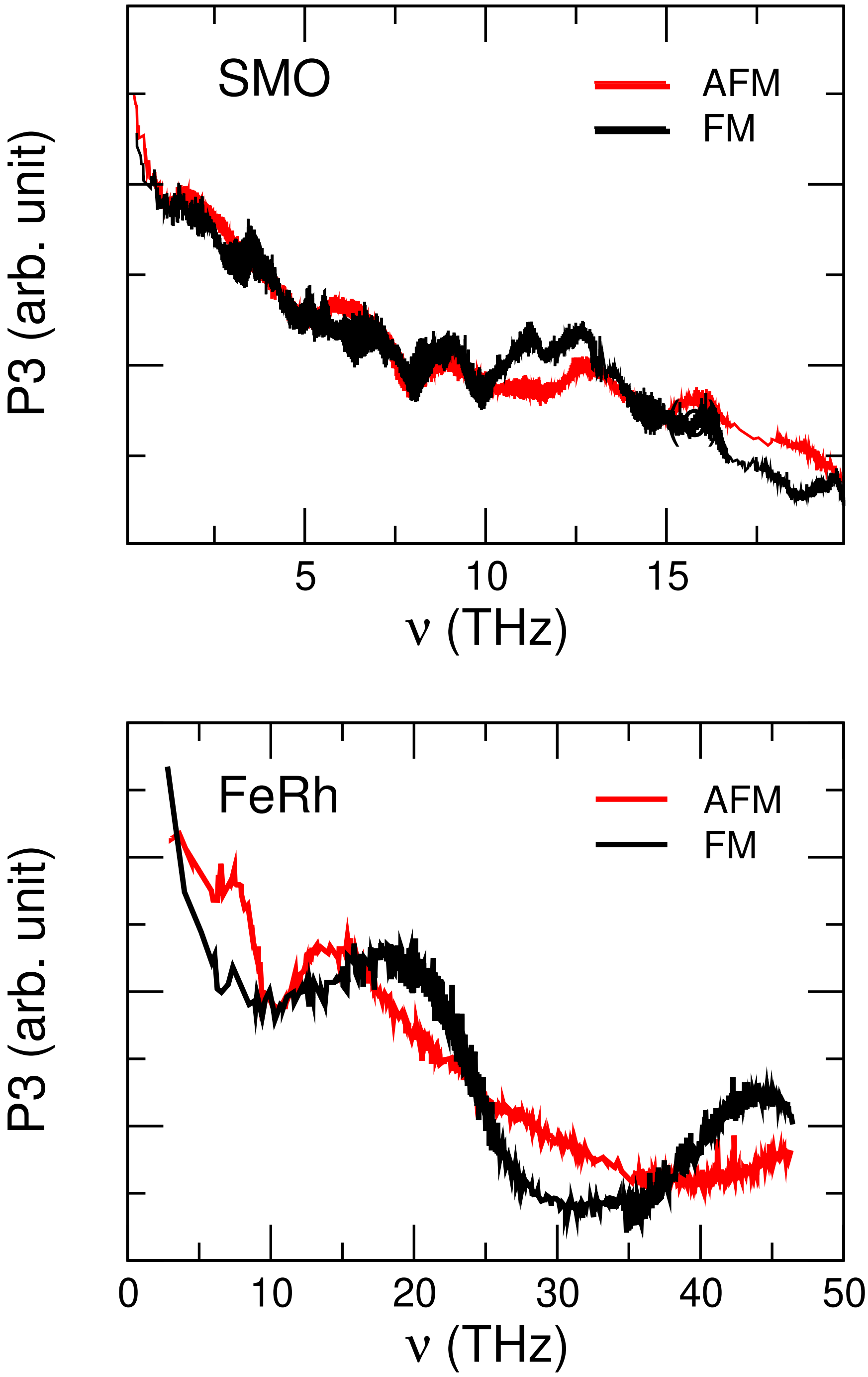

Supplementary Figure 8: Comparison between the phase-space volume for three-phonon collision process in the AFM and FM phases of SMO (this work) and FeRh [C. Cazorla and R. Rurali, Phys. Rev. B **105**, 104401 (2022)].